ISBN: 978-3-95450-199-1 doi:10.18429/JACoW-SAP2017-TUPH27

ELECTROMAGNETIC, THERMAL, STRUCTURAL ANALYSIS FOR THE RF-CAVITY OF A RHODOTRON ACCELERATOR *

L. Yang†, X. Z. He, H. Li, Institute of Fluid Physics, CAEP, Mianyang, Sichuan, China

Abstract

A Rhodotron-based electron accelerator served as micro-focused X-ray source at a high repetition rate of 10.75 MHz is proposed at IFP, CAEP. The RF-cavity, running in long pulse/ CW mode, will deliver 9 MeV energy gain to the charged beam at the exit by taking its advantage of multiple accelerations with the same field at a frequency of 107.5MHz. A substantial amount of power loss will be dissipated on the RF surface of the cavity within beam time. Further electromagnetic (EM) optimization was performed on a standard coaxial model with slight modifications aiming to achieve a higher shunt impedance, thus less power loss on surfaces. A proper water cooling design is still required to prevent large scale temperature rise on the cavity wall. The corresponding effects on cavity mechanical stability and resonant frequency shifting are concerned. This paper will present the details in the EM, thermal, structural analysis of the RF-cavity.

INTRODUCTION

Rhodotron, as a kind of compact electron accelerator with high efficiency of energy transfer to charged beams, has been widely employed to generate X-ray for industrial irradiation since the concept of multiple accelerations in the same field supplied by a half wave resonator (HWR) was raised by J. Pottier [1]. With several bend magnets azimuthally surrounding to an HWR, Electron beams could re-entry into the cavity and be re-accelerated at each time passing through a bend. A schematic view is shown in Figure 1. A high energy in the order of 10MeV which well meets the energy level of industrial irradiation sources, could be achieved with a relatively low field intensity. Hence long-pulse mode with large duty factor and fully continuous wave mode (CW) at an acceptable power loss level ~100kW are applicable and not often seen in normal conducting electron accelerators. Variable designs but in the same principle could be referred in these literatures [2-5]. We propose a micro-focused X-ray source at a high repetition rate of 10.75 MHz by adopting a 107.5MHz Rhodotron being able to accelerate electron beams with initial energy 40keV up to 9 MeV after 10 times across. Great efforts have been put on the beam dynamics design to form a 0.2 mm beam spot at the target location other than a typical size of 2 mm for normal industrial CT machines, which in details is documented in the paper ([6] A proposal of using improved Rhodotron as a high dose rate micro-focused X-ray source) of this conference. This paper is focusing on some specific cavity design issues.

One important thing should be carefully concerned is water cooling for CW running mode or high duty cycle mode. Large surface loss density in an order of 10^6 w/cm^2 is concentrated on the areas at the strong magnetic field zone considering OFC material being penetrated by RF field. Since the cavity body will be made out of stainless steel with OFC coated on the inner surface, the high surface loss density areas should be fully covered by forced water where efficient heat convection would occur. With the known heat convection status, one can perform the thermal analysis in those commonly used FEA codes to predict the steady temperature pattern over the cavity wall, which is of an important body load for the subsequent structural analysis and coupled thermal induced frequency drift estimation. The heat convection coefficient regarding to normal water cooling problems with regular meanders and uniform heat flux has been well developed in theory and usually adopted by the thermal simulations for normal conducting RF guns, cavities [7-8]. In our case, however, the heat convection highly depends on the local heat flux and varied fluid field due to the non-regular cavity geometry, therefore theoretical approximation is too roughly to calculate the distribution of heat convection coefficient. Thanks to the heat transfer enabled fluent package in ANSYS [9], the heat convection is internally computed and coupled with fluid calculation. The data mapping technology in Workbench allows load import between different physics fields that even don't share the same mesh and node pattern. By taking such advantages, we have done a complete coupled EM, thermal, fluid and structural simulation during the cavity design stage, which along with EM optimization will be presented in following sections.

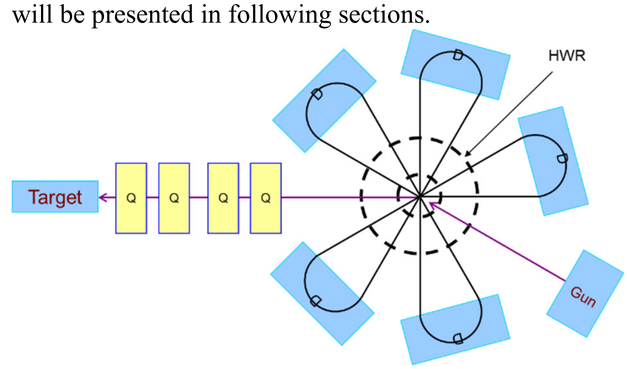

Figure 1: Layout of a Rhodotron.

EM OPTIMIZATION

EM optimization started with a standard initial coaxial line model resonating at the targeting frequency 107.5MHz. The outer conductor diameter **D** was set to 1.6m in order to keep an appropriate room for installing beam diagnostic elements on the beam line section between the cavity and the bend magnets. The inner conductor diameter **d** was defined to 0.25**D** where reaches the maximum shunt impedance by taking the transit time effect into account. A further optimization step with a

* Work supported by R&D project of IFP/CAEP
† yyperf57@163.com

ISBN: 978-3-95450-199-1 doi:10.18429/JACoW-SAP2017-TUPH27

cone feature and radial bend adding in the short ends was taken to get another 10% improvement on the shunt impedance. A longer cavity was resulted to fix the resonating frequency. This modification rather than a totally flat short plate, on the other hand, would increase the mechanical stability of the cavity. The whole set of RF parameters were calculated in HFSS. A wedge model (1/40 of the full model) was used for less mesh generation benefitting from symmetrical boundary conditions. Figure 2 shows the field patterns in the RF. Table 1 lists the comparison of key RF parameters and geometric parameters between the initial and final model.

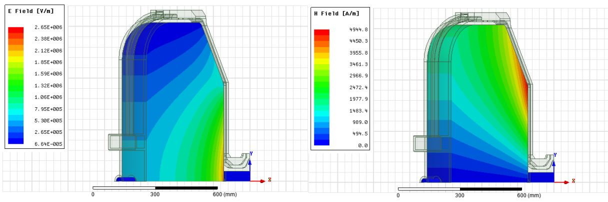

Figure 2: Electric field and magnetic field intensity. The cavity wall dressed with water cooling jacket appears as the transparent portion.

Table 1: RF Parameters and Key Geometric Parameters of the Initial, Final Models

Parameters	Initial model	Final model
Q_0(Copper)	42554	49086
Shunt impedance	10.6MΩ	11.8MΩ
Power loss	76kW	68kW
Cavity Height	1.39m	1.55m
Outer Diameter	1.6m	1.6m
Inner Diameter	0.4m	0.4m

COUPLED ANALYSIS

The complete coupled analysis engages 3 physics packages, EM, heat transfer enabled fluid and static structural with data links between each other to forecast the steady temperature rise in cavity body at a certain RF power level and flow rate of water, accordingly, the frequency shift due to thermal expansion, and the maximum thermal stress. All these packages are assembled in ANSYS, and should share the same model to carry out data access each other. A work flow is plotted in Figure 3 which also illustrates the data transfer network.

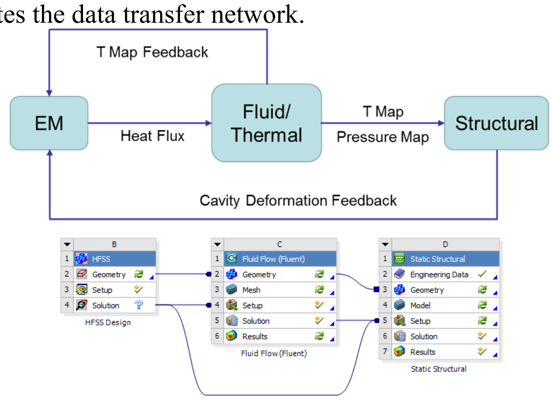

Figure 3: The work flow of the coupled analysis and a snapshot in ANSYS user interface.

The surface loss density calculated by HFSS is imported into Fluent as an energy source which will be conducted through the cavity wall in the solid zone and taken away by water flow in the fluid zone. The temperature distribution over the solid zone will be feedback to HFSS from Fluent. Since the resistance of the coated copper on the cavity inner surface is temperature dependent, an updated heat flux resulted from another run in HFSS will be reloaded into Fluent, and accordingly, the temperature distribution could be renewed. One can perform this iterative process couple times to meet the convergence threshold. In our case, single iteration has already shown a reasonable convergence. The final temperature distribution and the pressure load applied by the water flow will go forward into the static structural package. The deformation induced by thermal expansion and pressurized water and also the vacuum load in RF volume could be independently calculated or linearly superposed. The overall maximum stress is predicted by the latter one. The deformation will be captured by HFSS and mapped onto the mesh pattern for the new eigen mode calculation. The frequency shift is taking the difference to the initial eigen mode result.

Cooling Layout and Model Setup

The final RF model was translated into a shell model as the cavity wall with thickness of 15 mm, see Figure 4. The cooling layout over cavity wall was designed in a way that cooling efficiency and mechanical stability were both considered. The inner conductor and the short ends are fully covered by a jacket with a 5 mm gap, while the outer conductor is cooled by numbers of regular meanders evenly distributed along the cavity circumference. Pressurized water will be injected towards the blind plates in the medium region of the inner conductor. All the water flows drained out of these meanders are collected by a belt like buffer and circulated back to a chiller. These meanders play another import role of stiffening rings to keep the large cavity body rigid against water pressure, vacuum in RF volume, and thermal expansion. Similar to the EM calculation, symmetrical boundary conditions allow using a reduced model with water volume filled in all the gaps and meanders for the coupled simulation.

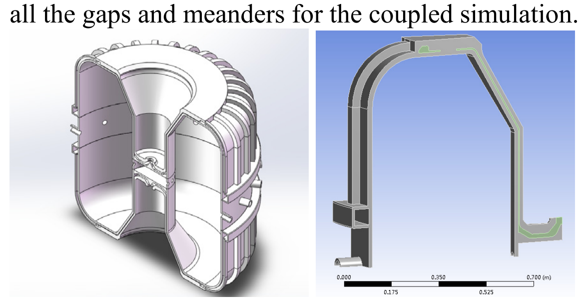

Figure 4: Left: Full cavity mechanical model; right: reduced model for coupled simulation, the water volume is coloured in green.

Simulation Setup and Single Pass Result

The field intensity in HFSS was adjusted to an overshot operational level (CW) with 15% margin to 68kW given

ISBN: 978-3-95450-199-1 doi:10.18429/JACoW-SAP2017-TUPH27

by the EM optimization as possible Q_0 degradation might take place during cavity fabrication. Temperature dependence of copper electric conductivity was enabled for the afterwards calculation with temperature feedback. The water flow rate was set to 55.7L/min which is equivalent to an average temperature rise of 10K at the outlet with respect to 77.5kW energy absorption by water. The water flow was injected at a typical temperature 300K. A rough estimation of Reynolds number in the areas with high flow velocities gives a range of 470~967. Hence, the fluid problem mostly falls in Laminar flow category (Re<2000). The configuration in Fluent doesn't require much attention to these complex models particularly solving turbulence problems. Large number of mesh in an order of million is required for a reasonable result even though a significantly reduced model was used. The RAM memory consuming is able to be handled by a modern desktop yet, and the time cost up to convergence is about 5 min, which is fairly acceptable.

After 40 iterations, the maximum temperature monitored in the entire processing reaches steady. The ramped up trace could be seen in Figure 5. The water temperature distribution in transverse plane on the outlet yields a mass-weighted average rise 9.94 K, and well consistent with the one predicted by a given flow rate. Figure 6 shows the temperature distribution with the initial heat flux load and the convection coefficient calculated from postprocessing. The coefficient varies in a broad range of -126.3 ~912.9 W/K·m^2, which is far beyond the estimations by theoretical models. The negative value means heat transfer back to some areas at low temperature. There are two regions with appreciable temperature rise, the one undergoing high loss density and the other one located in the medium of two adjacent meanders where water cooling doesn't reach and the heat has to be conducted away by stainless steel wall with poor thermal conductivity.

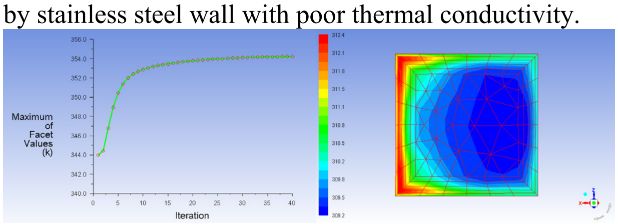

Figure 5: Left: maximum temperature trace over 40 iterations; right: water temperature distribution in transverse plane on the outlet.

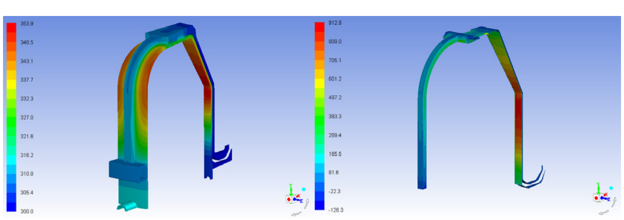

Figure 6: Temperature rise under initial heat flux load and the calculated convection coefficient

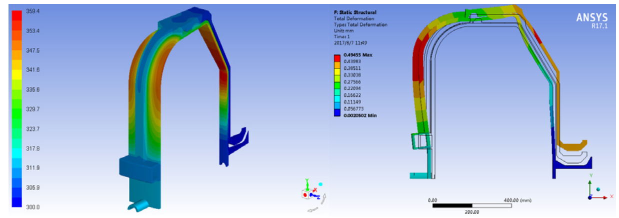

Figure 7: Updated temperature rise and induced deformation, note the frame in solid line is undeformed.

A 5% of Q0 drop after temperature feedback was seen, and in turn caused additional 5.6K (see Figure 7) rise to the initial maximum temperature, 353.9K. The heated cavity due to thermal expansion induces deformation with a maximum displacement of 0.495mm, and shifts the resonating frequency by a mount of -30.3 kHz to the one of a cold cavity.

Sweeping Flow Rate

More simulations have been done by sweeping the flow rate. The flow rate was adjusted from 27.9 to 139.3 L/min, coordinating to the mean temperature rise in fluid at the outlet, 4~20K. The maximum temperature and the induced frequency shift are plotted in Figure 8. When the flow rate is being increased over 60 L/min, the temperature drop starts to be slow down, where the high temperature spots on the outer conductor mainly cooled by thermal conducting become dominant. The optimized flow rate to this particular cooling layout, therefore could be defined at somewhere close to 60L/min.

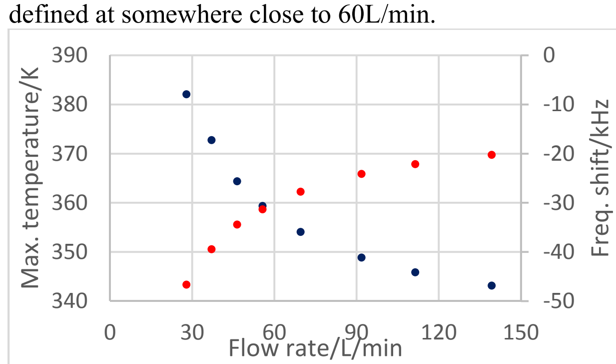

Figure 8: The maximum temperature (blue) varies with the flow rate and the corresponding frequency shift (red).

CONCLUSION

Calculation techniques for comprehensive EM, thermal, fluid and structural coupled simulation of RF cavities have been described extensively. Reasonable prediction on RF induced temperature rise is applicable owing to the heat transfer enabled fluid simulation with internally computation on the convection coefficient, which must have to be accurately given in advance in a sole thermal analysis. Cooling layout was severely designed for this specific RF cavity of a Rhodotron and verified in simulation with a controllable temperature rise at a full power level. The optimized flow rate to the cooling design has been forecasted by parameter sweeping.

ISBN: 978-3-95450-199-1 doi:10.18429/JACoW-SAP2017-TUPH27

REFERENCES

[1] J. Pottier *et al.*, "A new type of RF electron accelerator: the Rhodotron", *Nucl. Instrum. Methods-Phys.Res.B*, 40/41,p. 943, 1989.

[2] Y.Jongen *et al.*, "The Rhodotron: a 10 MeV, 100 kW beam power metric waves, CW electron accelerator", *Nucl. Instrum. Methods-Phys.Res.B*, 79, p.865, 1993.

[3] Abs M *et al.*, "The IBA Rhodotron T T1000: a very high power E beam accelerator", *Radiation Physics and Chemistry*, 2004, 71: 285-288.

[4] I. Jabbari *et al.*, "Design study of double-layer beam trajectory accelerator based on the Rhodotron structure", *Nucl. Instrum. Methods-Phys.Res.A*, 828, pp.72–80, 2016.

[5] R. Y. Song *et al.*, "Design of resonant cavity of petal shaped accelerator", *High power laser and particle beams*, Vol. 21, No. 12, Dec. , 2009.

[6] X. Z. He *et al.*, "A proposal of using improved Rhodotron as a high dose rate micro-focused X-ray source", presented at *Proc. SAP2017*, Jishou, China, 2017, this proceedings, paper TUPH08.

[7] F. Marhauser, "Finite Element Analyses for RF Photoinjector Gun Cavities", BESSY GmbH, Germany, TESLA FEL Report 2006 - 02.

[8] N. Hartman *et al.*, "Electromagnetic, Thermal, and Structural Analysis of RF Cavities Using ANSYS", in *Proc. PAC2001*, Chicago, USA, 2001, paper MPPH060, pp.912-914.

[9] ANSYS, http://www.ansys.com